Evaluation of Fibrin Clot Attachment on Titanium Laser-Conditioned Surface Using Scanning Electron Microscopy

Bruna Sinjari, DDS, Tonino Traini, MD, DDS,* Sergio Caputi, MD, DDS,* Carmen Mortellaro, MD, DDS,† and Antonio Scarano, MD, DDS‡*

Objectives: The study aimed to evaluate the effects of different titanium surface treatments on blood clot extension (bce).

Methods: A total of 54 titanium disks with machined surface (M), laser-conditioned surface (L), and grit-blasted surface (S) were used in the present study. The surface characteristics such as contact angles and the microroughness were determined on each group ($n = 4$). To evaluate the bce, 0.1 mL of human blood was dropped onto the surface of each specimen and left for 7 minutes at room temperature. After fixation, dehydration, and gold sputtering treatments, the specimens were observed under scanning electron microscope. The bce values were expressed as percentage of specimen surface covered by blood clot.

Results: The surface roughness (Ra ± standard deviation [SD]) was 0.75 ± 0.02 μm for M, 0.25 ± 0.02 μm for L, and 1.30 ± 0.03 μm for S. The contact angles measured in static conditions (WCA ± SD) were $71 \pm 5.4^\circ$ for M, $107 \pm 6.6^\circ$ for L, and $91 \pm 7.2^\circ$ for S. Regarding the bce (bce ± SD) of M samples ($65.5 \pm 4.3\%$) was statistically lower compared with both L ($83.4 \pm 5.1\%$) and S samples ($72.4 \pm 4.7\%$) ($P < 0.05$). Meanwhile, the L group showed the higher bce value.

Conclusion: The present results suggest that the laser-conditioned surface may increase the wettability and bce.

Key Words: Fibrin clot, implant surface, laser-conditioned surface

(*J Craniofac Surg* 2018;00: 00–00)

When a dental implant is placed in the bone, the surface first gets in contact with the blood originating from the injured vessels that meet and consequently the titanium (Ti) surface properties change. At the very first step, fast ionic macromolecular interactions happen. Usually, rapid adsorption of host plasma proteins such as immunoglobulins, vitronectin, fibrinogen, and fibronectin occurs on the implant surface, which leads to platelet adhesion. The latter triggers the coagulation of blood at the site of injury leading to thrombus formation.[1,2]

Fibrinogen, one of the most important proteins during coagulation, is the soluble blood precursor of the fibrin clot.[3] Both fibrinogen and fibrin play an important role in mediating clot formation, cellular and matrix interactions, fibrinolysis, inflammation, and wound healing.[3] The fibrin formation onto the implant surface almost immediately after insertion provides the temporary matrix to support the initial endothelial cell response needed for the vessel repair.[4]

Since migration of osteogenic cells is the hallmark of osteoconduction, both the formation of a fibrin scaffold and the activation of blood cells entrapped at the bone-implant interface can be expected to play a role in this first stage of the peri-implant bone healing cascade.[5] Several studies have been performed to better understand the factors that influence the bone healing cascades. Different researchers have reported that protein parameters as well as surface properties such as surface energy, roughness, and chemistry play a key role on the protein adsorption process.[6–8]

In fact, implant surface properties are likely to be of particular relevance to the chemical and biologic interface processes in the early healing stages after implantation. Schliephake et al (2005) showed that surface chemistry has the potential to alter ionic interactions, protein adsorption, and cellular activity at the implant surface.[9] These modifications may subsequently influence conformational changes in the structures and interactive natures of adsorbed proteins and cells.[10,11] Park and Davies (2000) found that plasma protein adsorption was increased on acid etched surfaces, thus enhancing the blood platelet aggregation on textured Ti surfaces.[12]

On the cellular level, biologic responses, such as the orientation and migration of cells and the cellular production of organized cytoskeletal arrangements, are directly influenced by the surface topography.[13] There is great evidence that surface roughness plays an important role in determining successful osseointegration of Ti implants.[14] Regarding the surface modifications, Di Iorio et al (2005) concluded that there is a correlation between implant surface morphology and fibrin clot extension. Improvement in surface microtexture complexity seems to determine the formation of a more extensive and three-dimensionally complex fibrin scaffold.[15]

Different techniques have been employed to alter and improve the surface topography; one of these is the laser-based technique.[16] The advantages of using lasers for surfaces treatment include the precise control of the frequency of the light, the high energy density, the ability to focus and raster the light, and finally the ability to control the reaction time. Laser treatment can be used for the specific tailoring of the surface features, even on different parts of the implants to induce different kinetics of bone formation.[17–19]

In a previous in vitro study, we reported an improvement of osteoblastic cell adhesion for laser-conditioned surface when compared with sandblasted and machined surfaces.[20] Moreover, in an

From the *Department of Medical, Oral and Biotechnological Sciences, University of Chieti-Pescara, Chieti; †Oral Surgery Unit, University of Piedmont, Novara; and ‡Department of Medical, Oral and Biotechnological Sciences and CeSI-MeT University "G D'Annunzio" of Chieti-Pescara, Chieti, Italy.

Received November 12, 2017.
Accepted for publication February 7, 2018.

Address correspondence and reprint requests to Antonio Scarano, MD, DDS, Via dei Vestini 31, 66100 Chieti, Italy;
E-mail: ascarano@unich.it

The authors report no conflicts of interest.

ISSN: 1049-2275
DOI: 10.1097/SCS.0000000000004519

animal study, it was reported an increase in bone implant contact rate for laser-treated surfaces.[21]

The blood/implant surface interaction should be considered the first step for osseointegration, unfortunately, it is not well understood, while, a better understanding could facilitate the control and predictability of dental implant success. This in vitro study was conducted to evaluate the fibrin clot adhesion on sandblasted, machined and laser-treated Ti implant disks with respect to their specific surface topography.

METHODS

General Procedure

A total of 54 disk-shaped, Ti samples with diameters of 5 mm and thicknesses of 2 mm with 3 different surface topographies (Geass, Pozzuolo del Friuli, Udine, Italy) were used in the present study. Of these, 30 were used for clot extension evaluation, 12 for surface analysis, and other 12 were for wettability analysis.

The specimens were divided as follows: 10 Ti specimens with machined surface (M), 10 Ti specimens with laser-conditioned surface (L), and 10 Ti specimens with grit-blasted surface (S). For all specimens, human whole blood without any addition of anticoagulant was employed. Venous blood was drawn from 3 healthy adult volunteers with a bleeding time from 2 to 3 minutes (Duke's assay), and 0.2 mL was immediately dropped onto the surface of each specimen with the use of a syringe. Because the blood drawn was instantly used for the experiment, the first drops were not discarded. The entire specimen surface could be covered with 0.2 mL of blood. Contact time was 5 minutes at room temperature; thereafter, the samples were rinsed with saline solution and fixed in a buffered solution at pH 7.2 of 2.5% of glutaraldehyde and 2.5% of paraformaldehyde. Samples were washed again with buffer and dehydrated in an ascending alcohol series of 50%, 70%, 90%, 95%, and 100%.

All the specimens underwent critical point drying in Emitech K 850 (Emitech Ltd, Ashford, Kent, United Kingdom) and treated for scanning electron microscope (SEM) examination as described above. After dehydration process, the specimens were mounted onto aluminum stubs, sputter gold coated in Emitech K 550 (Emitech Ltd) and observed by the use of a SEM (Zeiss EVO 50 XVP; Carl Zeiss SMY Ltd, Cambridge, United Kingdom) equipped with LaB6 electron gun and an Everhart-Thornley tetra solid-state detector (4Q-BSD). The SEM operating conditions included 5.0 kV accelerating voltage, 8 mm working distance, and a 5-pA probe current for high vacuum observations. Also a 25-kV accelerating voltage, 8.5 mm working distance, and a 250-pA probe current for observations under variable pressure (0.75 torr) were strictly used.

Specific Process Used to Produce the Different Surfaces

The M surface was related to machined implant surface, which was the condition that the surface came directly from the turning process (Geass).

Meanwhile, the S was based on grit-blasting procedure. Titanium surface after the turning process was subsequently treated with hard dry 100 mesh ultrapure Al_2O_3 at high velocity.

Laser micromachining was performed by means of a Q-switched DPSS Nd:YAG laser (355 mm wave length, 0.12 mJ/pulse energy, and 40 ns duration; Geass). Laser beam pulses produce a surface with thousands of hemispheric pores in less than a minute, which have a diameter of 20 μm an interpore distance of 30 μm and a hemispheric pore depth of 5 μm.

Measurements of Blood Clot Extension

A total of 30 disk-shaped samples were used for clot extension evaluation: 10 Ti specimens with machined surface (M), 10 Ti specimens with laser-conditioned surface (L), 10 Ti specimens with grit-blasted surface (S).

From each sample, 10 random micrographs at a magnification of 3000× were collected in .tif format with NxM 1024 × 768 grid of pixels using 4Q-BSD detector. To measure the areas covered by the fibrin clot, the images were analyzed using Image-Pro Plus version 6.0 (Media Cybernetics Inc, Bethesda, MD). To ensure accuracy, the software was calibrated for each experimental image using a software feature named "Calibration Wizard" which reports the number of pixel between 2 selected points (diameter of the disks). The linear remapping of the pixel numbers was used to calibrate the distance. The measurements drawn per each sample were then calculated for the group average. The blood clot extension (bce) values were expressed as percentage of specimen surface covered by blood clot.

Surface Characteristics Evaluation

Surface Topography

A Zeiss 510 meta confocal laser scanning microscope (CLSM; Zeiss, Jena, Germany) was used to measure the surface roughness. A total of 12 disk-shaped samples were used for surface topography evaluation: 4 Ti specimens with machined surface (M), 4 Ti specimens with laser-conditioned surface (L), and 4 Ti specimens with grit-blasted surface (S).

The area of measurement was 2 × 2 mm, and care was taken to choose the central area to avoid edge effects. The arithmetic mean of the profile points to the average line (Ra) was calculated for each sample. The surface topographic inspection was also conducted using SEM.

Surface Wettability

A total of 12 disk-shaped samples were used for surface wettability evaluation: 4 Ti specimens with machined surface (M), 4 Ti specimens with laser-conditioned surface (L), and 4 Ti specimens with grit-blasted surface (S).

The wettability was measured using the sessile drop method. For the evaluation, physiologic solution (Na-Cl 0.9%) was chosen, since it is similar to blood plasma in salt composition.

A 10-μL drop was carefully placed on each sample surface using a microsyringe. The analysis was made at room temperature 23°C (±2°C) under controlled humidity. Immediately after sample preparation, they were photographed using a high-resolution camera Nikon D800 (Nikon Imaging, Minato-Ku, Tokyo). The contact angle was measured from photographs, as the average of the left and right contact angle using a plugin of the software Image J (1.47 v Wayne Rasband, National Institute of Mental Health, Bethesda, MD).

Statistical Analyses

Statistical analysis was performed by means of a computerized statistical package (Sigma Stat 3.5, SPSS Inc, Ekrath, Germany). The data were analyzed with descriptive statistics to assess whether they had a normal distribution. One-way analysis of variance (ANOVA) and Holm-Sidak tests were used to evaluate the overall significance and to perform all pair-wise comparisons of the mean responses, respectively. The Pearson product moment correlation test was used to correlate the variables WCA, Ra, and bce for the different treatments. A P-value of <0.05 was considered statistically significant.

RESULTS

The surface SEM analysis of the M specimens showed the presence of typical machining grooves produced by the manufacturing instruments of turning process (Fig. 1A). Meanwhile, L specimens showed a very regular topography with pores of 20 to 25 μm of diameter and 5 to 9 μm of depth (Fig. 1B). The S showed a rough surface produced by the blasting procedure (Fig. 1C). The surface was irregular with many depressions, peaks, and small diameter indentations as typically for the sandblasted one. Under CLSM, the surface roughness (Ra ± standard deviation [SD]), was 0.75 ± 0.02 μm for M, 0.25 ± 0.02 μm for L, and 1.30 ± 0.03 μm for S surface. The ANOVA showed a significant difference among the groups ($P \geq 0.001$). Under multiple comparison procedure (Holm-Sidak test), all the difference appeared statistically significant ($P < 0.05$). The difference of Ra means between L and S was of 1.0 μm.

The contact angles measured in static conditions (WCA ± SD) was $71 \pm 5.4^\circ$ for M (Fig. 2), $107 \pm 6.6^\circ$ for L surface (Fig. 2), and $91 \pm 7.2^\circ$ for S (Fig. 2). The ANOVA discovered a significant difference among the groups ($P \leq 0.001$). The Holm-Sidak multiple comparison procedure showed a difference of WCA means between L and M of 36.1° ($P = 0.017$), while the difference of the means between L and S samples was 16° ($P = 0.05$).

The bce (bce ± SD) was $65.5 \pm 4.3\%$ for M, $83.4 \pm 5.1\%$ for L, and $72.4 \pm 4.7\%$ for S. The ANOVA discovered a significant difference among the groups ($P \leq 0.001$) (Fig. 3). The Holm-Sidak multiple comparison procedure revealed that bce of M samples was statistically lower compared with both L and S samples ($P \leq 0.05$). Also, statistical significant difference was noted between L and S samples ($P \leq 0.05$).

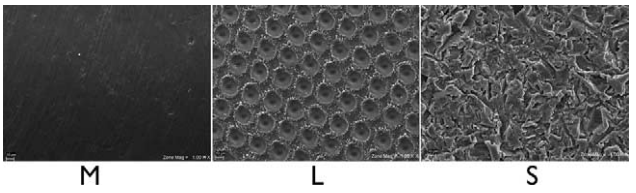

FIGURE 1. Scanning electron microscope analysis of M, L, and S surfaces at higher (1000×) magnifications.

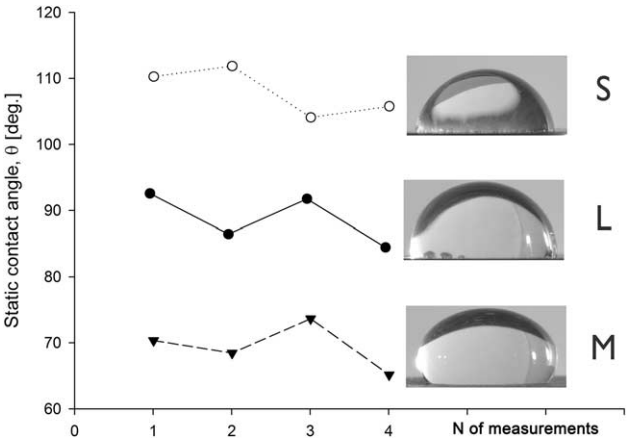

FIGURE 2. The contact angles measured in static conditions (WCA ± standard deviation). Note the presence of small air bubbles entrapped within the drop of M and S.

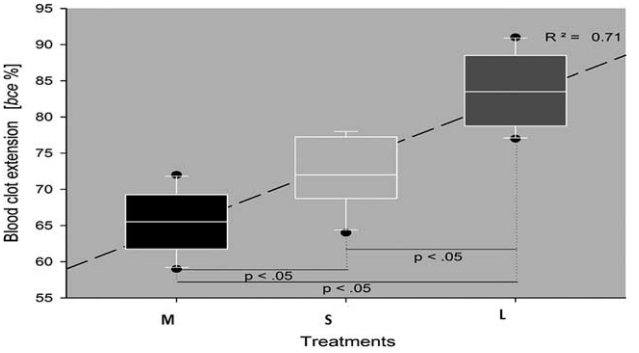

FIGURE 3. The box plot graphic shown a progressively incremental linear relationship of the blood clot extension passing, respectively, from M to S and to L.

The person product moment correlation considering the variables WCA, Ra, and bce for the different treatments does not show a significant relationship ($P > 0.05$).

Moreover, the SEM qualitative analysis showed differences in bce organization among all groups.

The SEM images of M specimens (Fig. 4 A-C) showed a thin fibrin scaffold attached to the specimen surface with a two-dimensional appearance (Fig. 3). On the contrary, L (Fig. 4 D-F) and S disks showed a three-dimensional organization of the fibrin scaffold (Fig. 4 G-I).

DISCUSSION

It is well established that characteristics of the implants surface, such as nano- and microtopography and physicochemical composition, have a major influence on the outcome of osseointegration, especially at the histological level, aiming at biologic and morphologic compatibilities.[22,23]

Following implant placement, the implant surface first gets in contact with the blood originating from the injured vessels facing the implant cavity. After several seconds, the surface is completely covered with a thin layer of serum proteins. This protein modification of the surface occurs for all implant materials in the same way. The results of present study showed that the implants with the

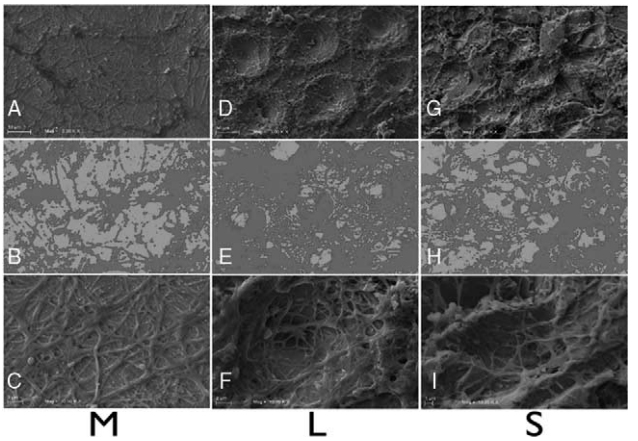

FIGURE 4. Scanning electron microscope (SEM) images of the blood clot extension of the M, L, and S(A-D-G; 3000× original magnification) using Image-Pro Plus version 6.0 images to measure the areas covered by the fibrin clot in red area and implant surface in green for the 3 surfaces (B-E-H). C-F-I: Higher magnification of titanium disks of the 3 surfaces on SEM (10,000× original magnification).

experimental surface L have a high wettability. Also the percentage of surface covered by the fibrin clot was very high in the L sample when compared to both M and S. Additionally, as shown in the box plot graphic (Fig. 3), a progressively incremental linear relationship passing, respectively, from M to S to L sample is present. These results suggest that increasing the complexity of the surface increases also the bce. In fact, the present results are in agreement with other studies in literature.[15,24] Di Iorio et al (2005) demonstrated that there is a positive correlation between implant surface morphology and fibrin clot extension. They also suggested that improvement in surface microtexture complexity seems to determine the formation of a more extensive and three-dimensionally complex fibrin network.[15]

The formation of the fibrin scaffold represents a transitory matrix; a real network which allows osteogenic cells migration through amoeboid movements, up to the implant surface, emphasizing the importance of the retention of fibrin by the implant surface.[5]

It has been demonstrated that the microstructure of the implant surface influences the degree of platelet activation during the clot formation, leading to a greater amount of chemotactic factors released during healing.[5] Thus, initial interactions of blood with an endosseous implant may influence clot formation and the eventual migration, and differentiation, of osteogenic cells in the healing compartment.

To alter the roughness of solid surfaces, a number of laser-based techniques have been applied in the past decades. The advantages of using lasers for the ablation of surfaces include the precise control of the frequency of the light, the wide range of frequencies available, the high energy density, the ability to focus and raster the light, and the ability to pulse the source and control the reaction time. Laser treatment can be used for the specific tailoring of the surface features, even on different parts of the implants to induce different kinetics of bone formation.[25]

On the contrary, the present Ra values reveal a surface roughness greater for S and M samples than for the L samples, while the bce was more extended on the L samples.

In that regard, it should be emphasized that the morphology of the surface, obtained by the laser technique, is represented by thousands of hemispherical flat concavity with a well-determined height and diameters and at the same time rougher interpore areas. Moreover, the laser surface treatment produces decontamination at surface in <1 minute, reducing both time and costs respect to the microsurface roughness devices traditionally prepared. In other words, it produces a microstructured surface at the microscale level with very smooth areas as shown by the present results.

On the contrary, the measurements of the contact angle showed a greater hydrophobicity for L samples, followed by S and M. Rupp et al (2004) shown that the microstructured surface gives rise to a 2-fold effect: an initial hydrophobicity, which is followed by an increased hydrophilicity.[26] This phenomenon seems to depend on small reductions of the contact angles, during the interaction with the liquid phase, by changing the initial wettability characteristics of the structures of hydrophobic surfaces.[26] The implant surface roughness and wettability have been considered as the most relevant aspects in establishing a clinically reliable bone attachment.[27]

Of course, such behavior cannot be studied with the sessile drop technique, characterized by a metastable equilibrium and simulating solid-liquid interface of constant hydrophobicity. In fact, the sessile drop is a static technique related to the disordered or Brownian movement of particles within the drop and to variables, represented solely by the pressure and the temperature. In contrast, the solid-liquid interface, at the peri-implant site, is a non-homogeneous environment, dynamic and transient one.

However, within the limits of the present study, it is demonstrated that the differences in surface morphology could explain the differences recorded in the extension of the fibrin clot, Ra, and WCA, indicating that these factors and their interaction may play an important role on the first steps of osteointegration such as fibrin clot formation and stabilization.

In addition to the present results, further studies are mandatory to better understand these complex phases of osteointegration and their role in de novo bone formation process after implant insertion.

REFERENCES

1. Keselowsky BG, Collard DM, Garcia AJ. Surface chemistry modulates focal adhesion composition and signaling through changes in integrin binding. *Biomaterials* 2004;25:5947–5954
2. Nygren H, Tengvall P, Lundstrom I. The initial reactions of TiO2 with blood. *J Biomed Mater Res* 1997;34:487–492
3. Hoppe B. Fibrinogen and factor XIII at the intersection of coagulation, fibrinolysis and inflammation. *Thromb Haemost* 2014;112:649–658
4. Kawase T, Okuda K, Wolff LF, et al. Platelet-rich plasma- derived fibrin clot formation stimulates collagen synthesis in periodontal ligament and osteoblastic cells in vitro. *J Periodontol* 2003;74:858–864
5. Davies JE. Mechanisms of endosseous integration. *Int J Prosthodont* 1998;11:391–401
6. Haynes CA, Sliwinsky E, Norde W. Structural and electrostatic properties of globular proteins at a polystyrene-water interface. *J Colloid Interface Sci* 1994;164:394–409
7. Deligianni DD, Katsala N, Ladas S, et al. Effect of surface roughness of the titanium alloy Ti-6Al-4 V on human bone marrow cell response and on protein adsorption. *Biomaterials* 2001;22:1241–1251
8. Michael KE, Vernekar VN, Keselowsky BG, et al. Adsorption-induced conformational changes in fibronectin due to interactions with well-defined surface chemistries. *Langmuir* 2003;19:8033–8804
9. Schliephake H, Scharnweber D, Dard M, et al. Functionalization of dental implant surfaces using adhesion molecules. *J Biomed Mater Res B Appl Biomater* 2005;73:88–96
10. Kilpadi DV, Lemons JE. Surface energy characterization of unalloyed titanium implants. *J Biomed Mater Res* 1994;28:1419–1425
11. Zhao G, Schwartz Z, Wieland M, et al. High surface energy enhances cell response to titanium substrate microstructure. *J Biomed Mater Res A* 2005;74:49–58
12. Park JY, Davies JE. Red blood cell and platelet interactions with titanium implant surfaces. *Clin Oral Impl Res* 2000;11:530–539
13. Flemming RG, Murphy CJ, Abrams GA, et al. Effects of synthetic micro- and nano-structured surfaces on cell behavior. *Biomaterials* 1999;20:573–588
14. Faeda RS, Tavares HS, Sartori R, et al. Biological performance of chemical hydroxyapatite coating associated with implant surface modification by laser beam: biomechanical study in rabbit tibiae. *J Oral Maxillofac Surg* 2009;67:1706–1715
15. Di Iorio D, Traini T, Degidi M, et al. Quantitative evaluation of the fibrin clot extension on different implant surfaces: an in vitro study. *J Biomed Mater Res B Appl Biomater* 2005;74:636–642
16. Bauerle D. *Laser Processing and Chemistry*. Berlin, Germany: Springer Verlag; 2000
17. Vorobyev AY, Guo C. Femtosecond laser structuring of titanium implants. *Appl Surf Sci* 2007;253:7272–7280
18. Brånemark R, Emanuelsson L, Palmquist A, et al. Bone response to laser-induced micro- and nano-size titanium surface features. *Nanomedicine* 2011;7:220–227
19. Hallgren C, Reimers H, Chakarov D, et al. An in vivo study of bone response to implants topographically modified by laser micromachining. *Biomaterials* 2003;24:701–710
20. Sinjari B, Guarnieri S, Diomede F, et al. Influence of titanium laser surface geometry on proliferation and on morphological features of human mandibular primary osteoblasts. *J Biol Regul Homeost Agents* 2012;26:505–513
21. Berardi D, De Benedittis S, Scoccia A, et al. New laser-treated implant surfaces: a histologic and histomorphometric pilot study in rabbits. *Clin Invest Med* 2011;34:E202
22. Scarano A, Degidi M, Perrotti V, et al. Experimental evaluation in rabbits of the effects of thread concavities in bone formation with different titanium implant surfaces. *Clin Implant Dent Relat Res* 2014;16:572–581

23. Scarano A, Perrotti V, Artese L, et al. Blood vessels are concentrated within the implant surface concavities: a histologic study in rabbit tibia. *Odontology* 2014;102:259–266
24. Traini T, Caputi S, Gherlone E, et al. Fibrin clot extension on zirconia surface for dental implants: a quantitative in vitro study. *Clin Implant Dent Relat Res* 2014;16:718–727
25. Branemark R, Emanuelsson L, Palmquist A, et al. Bone response to laser-induced micro- and nano-size titanium surface features *Nanomedicine* 2011;7:220–227
26. Rupp F, Scheideler L, Rehbein D, et al. Roughness induced dynamic changes of wettability of acid etched titanium implant modifications. *Biomaterials* 2004;25: 1429–1438
27. Scarano A, Piattelli A, Quaranta A, Lorusso F. Bone response to two dental implants with different sandblasted/acid-etched implant surfaces: a histological and histomorphometrical study in rabbits. *BioMed Res Int* 2017;2017:8724951